Response of Seasonal Simulations of a Regional Climate Model to High-Frequency Variability of Soil Moisture during the Summers of 1988 and 1993

SONG YANG

Climate Prediction Center, NOAA/NWS/NCEP, Camp Springs, Maryland

S.-H. YOO

RSIS/Climate Prediction Center, Camp Springs, Maryland

R. YANG AND K. E. MITCHELL

Environmental Modeling Center, NOAA/NWS/NCEP, Camp Springs, Maryland

H. VAN DEN DOOL AND R. W. HIGGINS

Climate Prediction Center, NCEP/NWS/NOAA, Camp Springs, Maryland

(Manuscript received 31 March 2006, in final form 7 March 2007)

ABSTRACT

This study employs the NCEP Eta Regional Climate Model to investigate the response of the model's seasonal simulations of summer precipitation to high-frequency variability of soil moisture. Specifically, it focuses on the response of model precipitation and temperature over the U.S. Midwest and Southeast to imposed changes in the diurnal and synoptic variability of soil moisture in 1988 and 1993.

High-frequency variability of soil moisture increases (decreases) precipitation in the 1988 drought (1993 flood) year in the central and southern-tier states, except along the Gulf Coast, but causes smaller changes in precipitation along the northern-tier states. The diurnal variability and synoptic variability of soil moisture produce similar patterns of precipitation change, indicating the importance of the diurnal cycle of land surface process. The increase (decrease) in precipitation is generally accompanied by a decrease (increase) in surface and lower-tropospheric temperatures, and the changes in precipitation and temperature are attributed to both the local effect of evaporation feedback and the remote influence of large-scale water vapor transport. The precipitation increase and temperature decrease in 1988 are accompanied by an increase in local evaporation and, more importantly, by an increase in the large-scale water vapor convergence into the Midwest and Southeast. Analogous but opposite-sign behavior occurs in 1993 (compared to 1988) in changes in precipitation, temperature, soil moisture, evaporation, and large-scale water vapor transport.

Results also indicate that, in regions where the model simulates the diurnal cycle of soil moisture reasonably well, including this diurnal cycle in the simulations improves model performance. However, no notable improvement in model precipitation can be found in regions where the model fails to realistically simulate the diurnal variability of soil moisture.

1. Introduction

It is widely recognized that, in addition to sea surface temperature (SST), soil moisture provides a strong forcing for governing atmospheric processes on various time scales (see reviews in Betts et al. 1996; Dirmeyer et al. 1999; Yang and Lau 2006; Koster et al. 2006). In the midlatitude continents, it may be the most important boundary condition during warm seasons (e.g., Koster and Suarez 1995; Lau and Bua 1998; Koster et al. 2000), especially in relatively dry regions (Xue et al. 1996). Although the variability of soil moisture is always considered a function of meteorological and hydrological

Corresponding author address: Dr. Song Yang, NOAA/Climate Prediction Center, 5200 Auth Road, Room 605, Camp Springs, MD 20746.
E-mail: song.yang@noaa.gov

DOI: 10.1175/JHM616.1

parameters such as precipitation and temperature, its influences associated with changes in the heat content of soil and evaporation feedback are linked not only to variations in local precipitation and temperature but also to remote climate anomalies via changes in temperature and pressure gradients, and thus atmospheric circulation (Pal and Eltahir 2002; Weaver 2004).

Soil moisture interacts with the overlying atmosphere through surface energy and water balances, and the amount of soil moisture strongly influences the degree of heat and moisture exchange between the land and the atmosphere (Qu et al. 1998; Dirmeyer et al. 2000; Timbal et al. 2002; Gutowski et al. 2004; Zhu and Liang 2005). As pointed out by Dirmeyer et al. (1999), soil moisture also determines the partitioning of land surface heat flux between sensible and latent components, thus affecting both heat and water balances. It influences conditions of overlying vegetation, determining transpiration and radiative properties. An increase in soil moisture weakens any increase in land surface temperature caused by solar radiation. On the other hand, it leads to increase in evaporation, which in turn strongly influences atmospheric convection and precipitation. The release of latent heat associated with the convection and precipitation enhances low-level moisture convergence and thus further intensifies precipitation (e.g., Lau and Bua 1998).

Development of convection associated with the changes in atmospheric moisture or surface temperature modulated by soil moisture causes anomalies in atmospheric circulation. While previous studies often focus on the anomalous atmospheric circulation of mesoscales (Segal et al. 1995; Eltahir 1998; Baker et al. 2001), it should also be realized that the change in temperature may modify the gradients of temperature and pressure over broad regions and these modified broad-scale gradients may change large-scale patterns of atmospheric circulation.

Soil moisture also influences precipitation, temperature, and atmospheric circulation through the "reservoir" or "land memory" effect. This effect has been demonstrated by the relationships between warm-season precipitation and the soil moisture that exists before the warm season, which is often related to antecedent snow accumulation. These relationships are evident in the connection between summer monsoons and the preceding snow cover in Asia as well as in North America (Hahn and Shukla 1976; Barnett et al. 1989; Meehl 1994; Yang et al. 1996; Gutzler and Preston 1997; Higgins et al. 1998; Yang and Lau 1998; Hu and Feng 2002). Even in the summer season itself, the monthly persistence of surface temperature cannot be well explained without soil–atmosphere interactions (Huang and Van den Dool 1993; Huang et al. 1996).

Previous studies have also demonstrated the importance of soil moisture initialization for climate modeling (e.g., Smith et al. 1994; Koster and Suarez 1995; Betts et al. 1996; Fennessy and Shukla 1999; Koster et al. 2004). In particular, Koster et al. (2004) have shown an increase in precipitation forecast skill by realistic initialization of soil moisture and other land surface state variables especially in May through July. Accumulated evidence has indicated that reductions in errors of soil moisture initialization in models improve the ability of the models in climate simulation and prediction (e.g., Mahanama and Koster 2005).

Thus, the impacts of soil moisture on the atmosphere result in various atmospheric processes of different temporal and spatial scales. While analyses of the surface flux budget and energy balance often focus on the effect of soil moisture on relatively high frequencies, the studies of the memory effect of soil moisture usually target longer time scales. Within this context, many issues about the multiscale effects of land–atmosphere interaction remain unclear, for example, what are the impacts of the high-frequency variability of soil moisture on the low-frequency variations of precipitation, temperature, and atmospheric circulations?

The above review concludes that soil moisture affects precipitation, temperature, and atmospheric circulation relatively simultaneously via its effect associated with surface energy balance, and less concurrently through its memory effect. These effects of soil moisture can be both local by modifying surface energy flux and remote by changing temperature and pressure gradients over large regions, and thus changing the atmospheric circulation. Because of these soil moisture influences, realistic initialization of land surface states in models is important for realistic climate simulations. The discussion within this context raises another question: How will model results vary with changes in the frequency of updating land surface states as surface boundary forcing?

In this study, we investigate the response of model-simulated atmosphere, especially the response of seasonal precipitation and temperature, to the high-frequency variability of soil moisture using the National Centers for Environmental Prediction (NCEP) Eta Regional Climate Model (Eta Model). We investigate the summers of 1988 and 1993 when very different hydroclimate conditions emerged. The contiguous United States experienced the warmest and driest climate conditions in decades in summer 1988 and one of the most devastating floods in modern history in summer 1993.

These extreme climate events caused large losses for agriculture and human lives and property. The summers of 1988 and 1993 are also characterized by very different processes of land surface hydrology, and thus different features of land–atmosphere interaction. Therefore, the two summers have been the subject of many studies focusing on drought and floods (Namias 1991; Beljaars et al. 1996; Trenberth and Guillemot 1996; Xue et al. 1996; Viterbo and Betts 1999; Hong and Kalnay 2000; Pal and Eltahir 2001; among many others). The emphasis of our study is on the response of the model to the diurnal and synoptic variability of soil moisture and on an assessment of the importance of frequent updates of soil moisture as surface boundary forcing for climate modeling.

In the next section, we provide a description of the model, design of model experiments, and methods of analysis. In section 3, we compare model output with observations and explore the features associated with the changes in precipitation and temperature caused by the diurnal and synoptic variability of soil moisture. In section 4, we attempt to explain these features by local evaporation effect and remote atmospheric circulation effect and discuss the strengths and weaknesses of this study. A summary of the study is given in section 5.

2. Model, experiments, and analysis methods

The NCEP Eta Model was configured from the operational mesoscale numerical weather forecast model of NCEP from the early 1990s until late June 2006, with various model upgrades periodically implemented throughout that time. Such regional climate model (RCM) configurations of the Eta Model have been applied in several regional climate model studies (Takle et al. 1999; Fennessy and Shukla 2000; Xue et al. 2001). The particular version of the model used in this study is very close to the version used in the NCEP North American Regional Reanalysis (NARR; Mesinger et al. 2006). Specifically, it is the RCM-configured version of the Eta Model executing operationally at NCEP in November 2001. With respect to the latter numerical weather prediction version, we made traditional changes to achieve the RCM configuration, namely, to enable longer-period model integrations and to invoke daily updates of (i) SST and sea ice from external analyses and (ii) fraction of green vegetation cover and albedo from temporal interpolation of monthly climatologies.

The Eta Model reduces errors in the pressure gradient force over steeply sloped terrains with accurate treatment of complex topography using Eta vertical coordinate (also referred to as "step mountain" vertical coordinate). The Eta Model employs the semistaggered Arakawa E grid in which wind points are adjacent to mass points, configured in rotated spherical coordinates. The model physics, largely described by Janjić (1990, 1994), includes a modified Betts–Miller scheme for deep and shallow convection. The scheme for explicitly predicted cloud water employs the scheme of Zhao and Carr (1997). The Geophysical Fluid Dynamics Laboratory (GFDL) scheme is used for radiation. Free atmospheric turbulent exchange above the lowest model layer is via Mellor–Yamada level 2.0 (Mellor and Yamada 1982), and the treatment of the surface layer and similarity functions therein is described in Chen et al. (1997). A viscous sublayer is used over water surface. The land surface model is the NCEP Noah land surface model (Chen et al. 1997; Ek et al. 2003), which is a modified version of the Oregon State University land surface scheme. The Noah model has four soil layers: surface to 10, 10–40, 40–100, and 100–200 cm. The spatial resolution and large domain of the Eta Model used in this study are identical to those used in NARR, namely, 32 km in the horizontal, with 45 levels in the vertical, and a domain spanning 10°–90°N, 164°–58°W. If we had used a smaller model domain, that would have increased the control by the lateral boundary conditions, thereby constraining internal variability and weakening the effect of soil moisture variability. Also as in NARR, we specify the temporal lateral boundary conditions from the NCEP/Department of Energy (DOE) Global Reanalysis II (Kanamitsu et al. 2002). Our approach is consistent with the approach taken by many previous RCM studies, wherein observed SST and global reanalysis are used as the source of time-dependent sea surface and lateral boundary conditions (see Takle et al. 1999).

Using the Eta Model described above, we first conduct seasonal control simulations for the warm seasons of 1988 and 1993. For each year, we use the data of Global Reanalysis II as the initial atmospheric conditions for five ensemble members launched from the 0000 UTC data of 26–30 April. For all experiments, we integrate the model for more than four months (until early September), longer than most of the integrations of previous studies that used the Eta Model in RCM mode. Initial snow depth is from a U.S. Air Force daily analysis and all remaining initial land states including soil moisture are from NARR. Output of the control simulations, including soil moisture, is saved every three hours for analysis and subsequent use in sensitivity experiments.

We devote more effort to the sensitivity experiments, which are classified into three groups: 3H, D, and W.

The only difference among these sensitivity experiments from the control simulations occurs in the treatment of soil moisture. Before conducting these experiments, we construct the ensemble means of 3-hourly soil moisture from the output of control simulations and compute the daily and weekly averages from these ensemble means. During model execution in experiments 3H we impose the 3-hourly ensemble-mean soil moisture from the control simulations. Similarly, we use the daily means and weekly means of soil moisture to force the model in experiments D and W, respectively. There are five ensemble members for each group of the sensitivity experiments from the same five initial dates given earlier.

To assess the impact of the diurnal variability of soil moisture on precipitation and other fields, we analyze the difference between experiments 3H and experiments D (hereafter 3H-D). To measure the impact of the synoptic variability of soil moisture, we analyze the difference between experiments 3H and experiments W (hereafter 3H-W). Thus, 3H-W measures the influences of the variability of soil moisture on synoptic and subsynoptic time scales, although it is referred as to synoptic variability of soil moisture for convenience in this study.

3. Results

a. Control simulations and comparison with observations

To assess the performance of the model, we compare the ensemble means from the control simulations described above and several products of analysis or reanalysis. These products include the NCEP Climate Prediction Center (CPC) Unified Precipitation Analysis (Higgins et al. 2000), NCEP Regional Reanalysis (Mesinger et al. 2006), and NCEP Land Data Assimilation System (NLDAS; Fan et al. 2006). To evaluate model performance against observations, one may compare the total values or the anomalies of individual fields. However, as in many previous studies (e.g., Fennessy and Shukla 2000; Palmer et al. 2004; Saha et al. 2006), model performance is often evaluated by examining anomaly fields because model climates are usually different from the observed. Furthermore, we only conduct simulations for two years (1988 and 1993) and are unable to construct model climatology for computing the anomalies. Thus, we compare the difference fields between the two years, as in Fennessy and Shukla (2000) and others.

Figure 1 shows the difference (1993 minus 1988) in June–August (JJA) precipitation for the CPC's unified precipitation analysis and for the Eta Model. From the

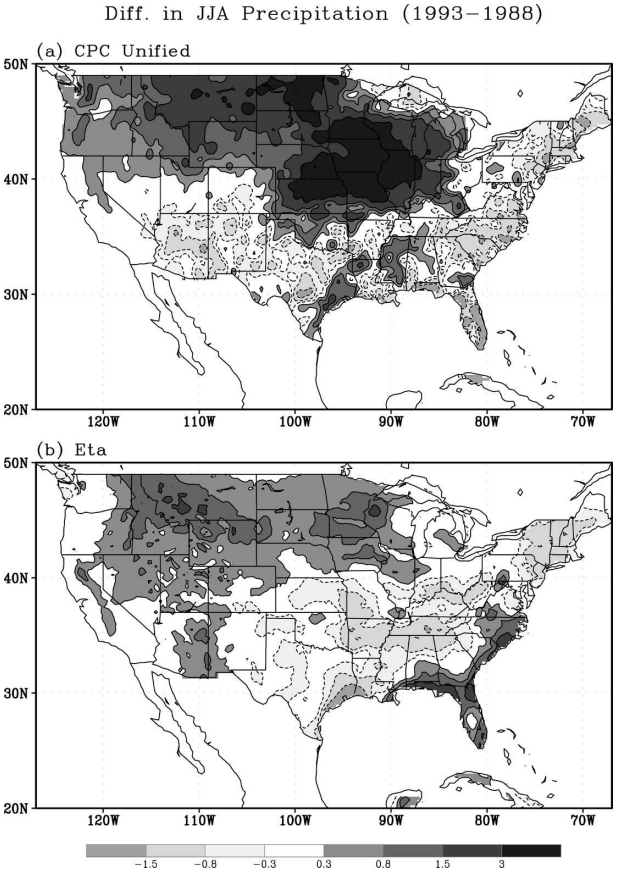

FIG. 1. Differences in JJA precipitation (mm day^{-1}) between 1993 and 1988 in (a) the National Oceanic and Atmospheric Administration (NOAA)/CPC unified precipitation product and (b) the ensemble means of Eta control simulations. Dashed contours are for negative values.

analysis (Fig. 1a), positive values (more precipitation in 1993 than in 1988) appear in the northern-tier states (e.g., 40°N and northward), except the Northeast and the Midwest. On the other hand, negative values appear in most of the southern-tier states with weaker magnitude and mixed signals in some places. Broadly speaking, in terms of the positive–north and negative–south patterns, the Eta Model captures the observed features reasonably well (Fig. 1b). Closer inspection reveals that the model performs better for the regions north of 40°N than those to the south. For example, there is fairly good agreement between the results of model and analysis over the Northeast, but the model does not realistically simulate the observed difference in the monsoon precipitation over the Southwest. According to Koster et al. (2006, see their Fig. 2), the southwest monsoon region is not a "hot spot" of precipitation sensitivity to soil moisture and hence the unrealistic Eta precipitation simulation over the region is

not a focus of this study. In the Midwest, there is a notable discrepancy between model and observations across an east–west belt spanning Kansas and Indiana, reflecting the fact that the model displaces the southern edge of positive anomalies too far north. Several previous studies (e.g., Beljaars et al. 1996; Viterbo and Betts 1999; Fennessy and Shukla 2000) have also reported that the positive precipitation anomaly associated with the 1993 Midwest flood produced by various models is too northward compared to the observed. Nevertheless, the studies of Beljaars et al. (1996) and Viterbo and Betts (1999) are also soil moisture sensitivity studies (though not studies of sensitivity to temporal variability) and they are widely considered pillar studies of soil moisture sensitivity. Similarly, here in our study, in spite of the northward bias in our control, we believe that the associated sensitivity experiments, which will be presented in sections 3b, 3c, and 4, are warranted and have merit.

In Fig. 2, we show the patterns of 500-mb geopotential height (H500), for a larger domain, to reveal the features in large-scale atmospheric patterns. In the reanalysis (Fig. 2a), a difference low (smaller H500 in 1993 than in 1988) is located over the northern Great Plains and near the U.S.–Canada border and a difference high to its Southeast centered over Louisiana and Alabama. Thus, compared to 1988, anomalous southerly winds prevailed over the south (implying larger water vapor supply from the western Gulf of Mexico) and the Northeast and anomalous westerly winds over the central United States in 1993. The Eta Model captures this north–low and south–high pattern and thus the Northwest–Southeast pressure gradient. The model also captures the high and low patterns over the eastern Pacific. However, the major difference low over the U.S.–Canada border is located too northward, over the Canada territory in the model. Overall, the Eta Model produces weaker-than-observed atmospheric circulation patterns between the two years, consistent with the patterns of model precipitation (Fig. 1) and temperature (Fig. 3). It should be pointed out again that we executed the Eta domain over a large domain (10°–90°N, 164°–58°W) for this study to let the Eta simulation not be overly controlled by the lateral boundary conditions, and hence the simulated height does not preserve the North American height pattern of the global reanalysis from which the lateral boundary conditions were obtained.

The summer of 1993 was generally colder than the summer of 1988 except in some southern-tier states (e.g., New Mexico, Texas, and Arkansas) and the Southeast coastal regions, as shown by the difference in

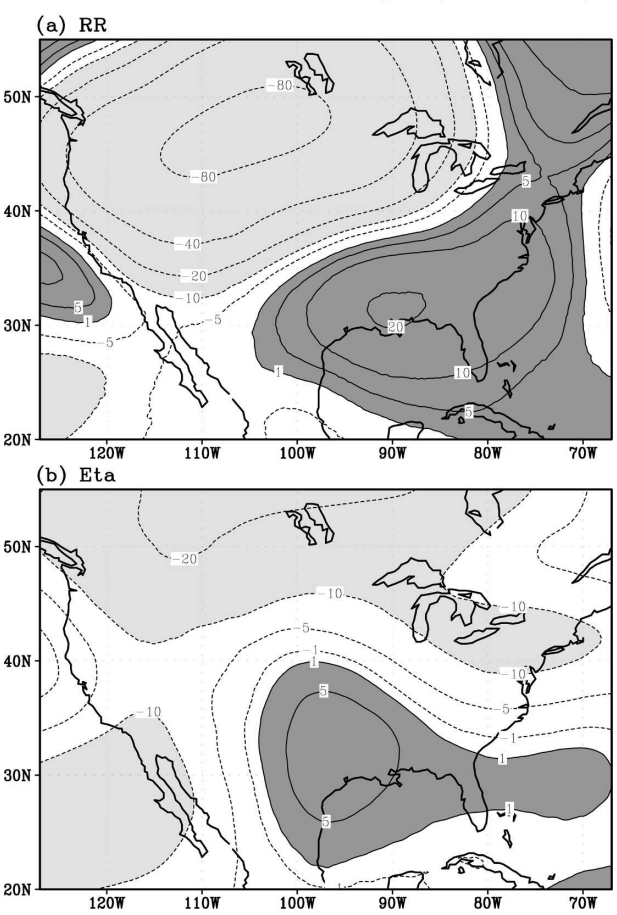

FIG. 2. Differences in JJA 500-mb geopotential height (m) between 1993 and 1988 in (a) the NCEP Regional Reanalysis and (b) the ensemble means of Eta control simulations.

land surface temperature (Fig. 3a). The Eta Model simulates these features reasonably well except for the Southeast coasts and Texas (Fig. 3b), despite Fig. 3 showing generally weaker amplitude of difference in the simulated temperature between the two summers. There is also consistency between the reanalysis and simulation patterns of sensible heat flux (Figs. 3c,d). In both Eta and reanalysis products, large positive (negative) values of temperature difference are accompanied by positive (negative) values of sensible heating difference. A comparison between Figs. 1 and 3 indicates that the model simulates the temperature difference better than the precipitation difference, consistent with the result of Fennessy and Shukla (1999, 2000).

Figure 4 displays the difference in the depth of JJA soil moisture between 1993 and 1988 in the NCEP Land Data Assimilation System and in the Eta Model. As shown in the assimilated data (Fig. 4a), most of the United States was generally wetter in 1993 than in 1988.

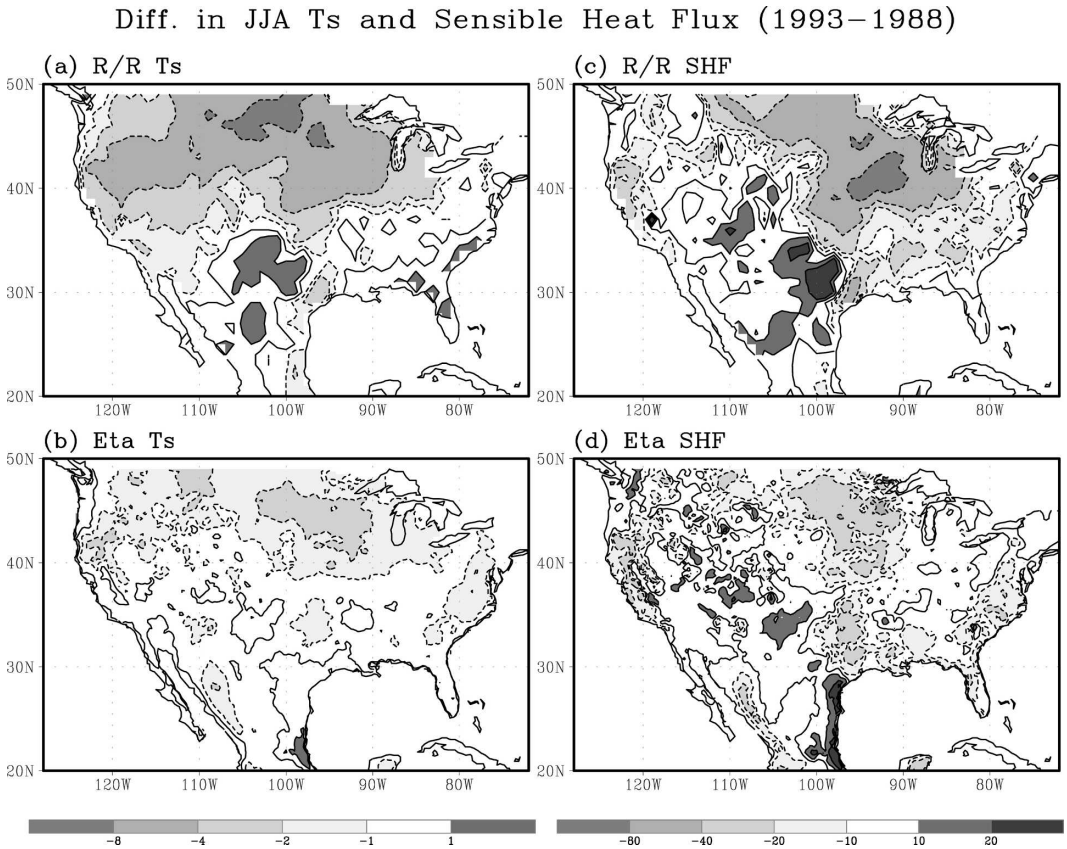

FIG. 3. Differences in JJA land surface temperature (°C) between 1993 and 1988 in (a) the NCEP regional reanalysis and (b) the ensemble means of Eta control simulations. Shown also are the differences in JJA sensible heat flux (W m^{-2}) between 1993 and 1988 in (c) the NCEP regional reanalysis and (d) the Eta ensemble means. Zero contours are drawn and dashed contours are for negative values.

The Eta Model (Fig. 4b) captures many features shown in Fig. 4a and performs better for the western United States and east of 95°W except the East Coast. As in the patterns of precipitation, geopotential height, and temperature (Figs. 1–3), the Eta Model produces smaller differences in soil moisture between the two summers compared to the assimilated data.

We have also examined the daily mean sea level pressure averaged over 20°–55°N, 130°–65°W for 1988 and 1993 from the control simulations and the NCEP regional reanalysis (figures not shown). The simulated values (ensemble means) are significantly correlated with those in the regional reanalysis. The correlation coefficients between the two are 0.50 for 1988 and 0.42 for 1993, exceeding the 99% confidence level of *t* test. There is also consistency in the variability of sea level pressure among the various ensemble members. In addition, we examine the patterns of signal-to-noise ratio as defined by Stern and Miyakoda (1995) as "reproducibility" for the patterns of geopotential height, precipitation, temperature, and soil moisture shown in Figs. 1–4. In each case, the signal is larger than the noise (spread) for the majority of the United States.

As described in section 2, in this study the 3-hourly ensemble means of soil moisture from control simulations are used as the forcing for sensitivity experiments. Figure 5 shows the depth of soil moisture at 42°N, 93°W for experiments 3H, D, and W, and for 1988 and 1993, respectively. (More details of spatial patterns of the diurnal cycle of soil moisture are discussed in Figs. 17 and 18.) The figure reveals large differences among the data series of different time scales but of the same data source. It also indicates that soil moisture is more variable in the 1988 drought year than in the 1993 wet year. (The decrease in soil moisture with time is part of the annual cycle.) In spite of substantial spatial variability, apparent differences in soil moisture of different temporal scales also exist in other grid points. However, area averages reduce these differences as expected. This suggests a need of future studies to understand the impact of soil moisture variability of different spatial scales on precipitation variations.

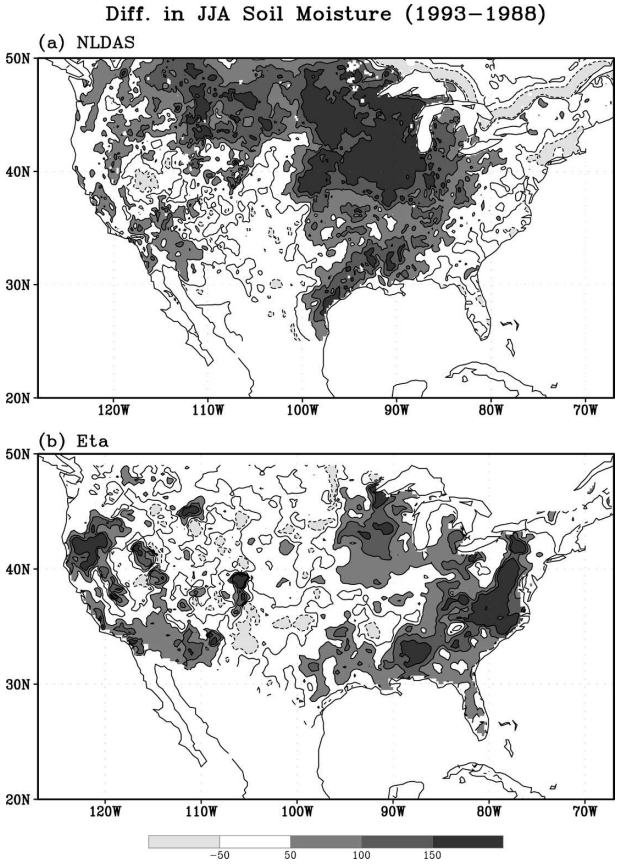

FIG. 4. Differences in depth of JJA soil moisture (mm) between 1993 and 1988 in (a) the NLDAS and (b) the ensemble means of Eta control simulations (summation of four layers). Zero contours are drawn and dashed contours are for negative values.

b. Response of precipitation and temperature to the diurnal and synoptic variability of soil moisture

In this section, we explore features associated with the impact of diurnal (synoptic) variability of soil moisture on seasonal precipitation and temperature by analyzing the difference between experiments 3H and D (3H and W). We analyze the ensemble means of these sensitivity experiments.

1) YEAR OF 1988

Figure 6 shows the patterns of JJA precipitation in experiments 3H and precipitation differences in 3H-D and in 3H-W for 1988. Figure 6a, which yields a similar precipitation pattern to that of the control simulations (not shown), illustrates a large amount of precipitation in the eastern United States and a general decrease in precipitation from the east to the west. In most of the Midwest, the precipitation rate ranges from 2 to 4 mm day^{-1}.

It can be seen from Fig. 6b that the diurnal variability of soil moisture increases the model precipitation in JJA 1988 over much of the United States except the Great Lakes, Northwest, and southern Texas. The enhancement of precipitation is largest in the fourth quadrant. In the Southeast and part of the Midwest, precipitation increases significantly by more than 0.5 mm day^{-1}, a large number that is about 20% of the total precipitation. The pattern of Fig. 6c is more significant than that of Fig. 6b. Overall, it resembles Fig. 6b, except for Colorado, Wyoming, and part of the northern Midwest. The similarity between Figs. 6b and 6c indicates the importance of the diurnal variability of soil moisture for precipitation variations.

For 1988, the 3-H experiments yield high temperature over the Southwest and central United States and cold temperature in the northeastern part and west coast of the country and the eastern Rocky Mountains (Fig. 7a). Associated with the changes in precipitation shown in Figs. 6b,c, strong signals appear in the difference in surface temperature because of the impact of soil moisture (Figs. 7b,c). Overall, the high-frequency variability of soil moisture decreases model temperature in most of the central and eastern United States (east of 105°W) except Texas, and increases the temperature in the west. In some regions, changes in temperature are as high as 0.5°–1.0°C. Like the features shown in precipitation, the diurnal variability and synoptic variability of soil moisture lead to generally similar patterns of change in surface temperature except in Texas and part of the four-corners states (Arizona, New Mexico, Colorado, and Utah). The changes in temperature are not limited to the earth's surface but also extend to the lower troposphere (figures not shown).

Figure 8 shows the seasonally averaged daily variances of precipitation and temperature and their changes with soil moisture forcing in various experiments. The daily variances are computed as the daily perturbations (mean squares) of precipitation and temperature from their seasonal means. In experiment 3H, the model produces larger (smaller) precipitation variance to the east (west) of about 95°W (see Fig. 8a). The largest temperature variance is over the west and then the northern-tier states, and the lowest values appear over the Gulf Coast and Southeastern states (Fig. 8d). While mixed signals appear over the western part of the country, the diurnal and synoptic variability of soil moisture leads to increase in daily variability of precipitation over the central-eastern United States. The high-frequency variability of soil moisture enhances the temperature variability over the southern-tier states west of

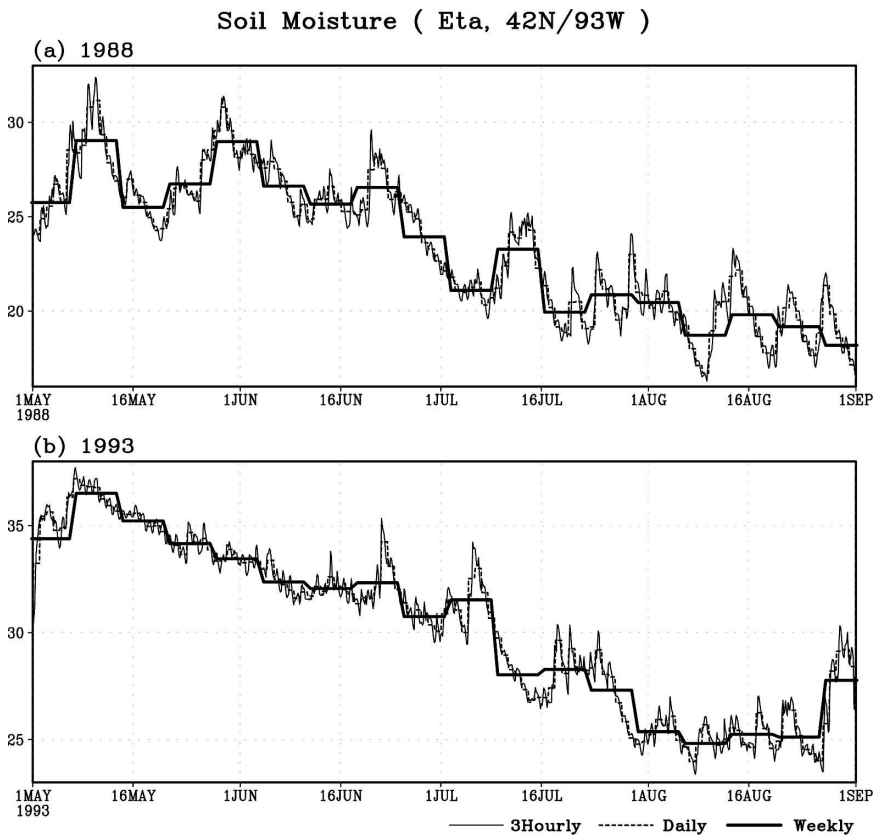

FIG. 5. Time series of Eta ensemble-mean depth of soil moisture (top layer; units: mm) at 42°N, 93°W for (a) 1988 and (b) 1993. The values, shown for 3-hourly, daily, and weekly, are from the control simulations and the values of each layer are also the forcing functions at the specific grid point for the sensitivity experiments 3H, D, and W, respectively.

90°W and weakens the temperature variability to the north and east, with mixed features over the Gulf Coast states. A comparison of Figs. 6b,c with Figs. 8b,c indicates that the high-frequency variability of soil moisture causes similar changes in mean precipitation and precipitation variance. That is, large (small) precipitation variance coexists with increase (decrease) in the mean precipitation. However, no such relationship can be clearly seen between the mean temperature and temperature variance.

2) YEAR OF 1993

The response of precipitation to the diurnal and synoptic variability of soil moisture in JJA 1993 is shown in Fig. 9. Again, the influence of diurnal variability is measured by the difference between experiments 3H and D, and that of synoptic variability by the difference between experiments 3H and W. Figure 9b shows that the diurnal variability of soil moisture decreases the model precipitation of 1993 over much of the United States except the east coast regions, the Great Lakes, the Northwest, and the Southwest. Maximum decrease in precipitation appears in the Midwest, the Ohio Valley, and the northern Southeast. Figure 9c indicates that the changes in precipitation caused by synoptic variability of soil moisture are generally similar to those caused by the diurnal variability of soil moisture. The general decrease in central U.S. precipitation for 1993 shown in Figs. 9b,c is different from the general increase in precipitation for 1988 shown in Figs. 6b,c.

It can be seen from Fig. 10 that, for JJA 1993, the high-frequency variability of soil moisture increases surface model temperature in most of the United States except the Northwest and Gulf Coast (as well as the southern Midwest in Fig. 10b). In particular, temperature increases clearly in the central United States, including the Great Plains and northern Midwest. As for 1988, the diurnal and synoptic variability of soil moisture leads to generally similar patterns of temperature changes for 1993 (cf. Figs. 10b,c). Also, the features shown in Fig. 10 are similar to the features of 850-mb temperature (not shown).

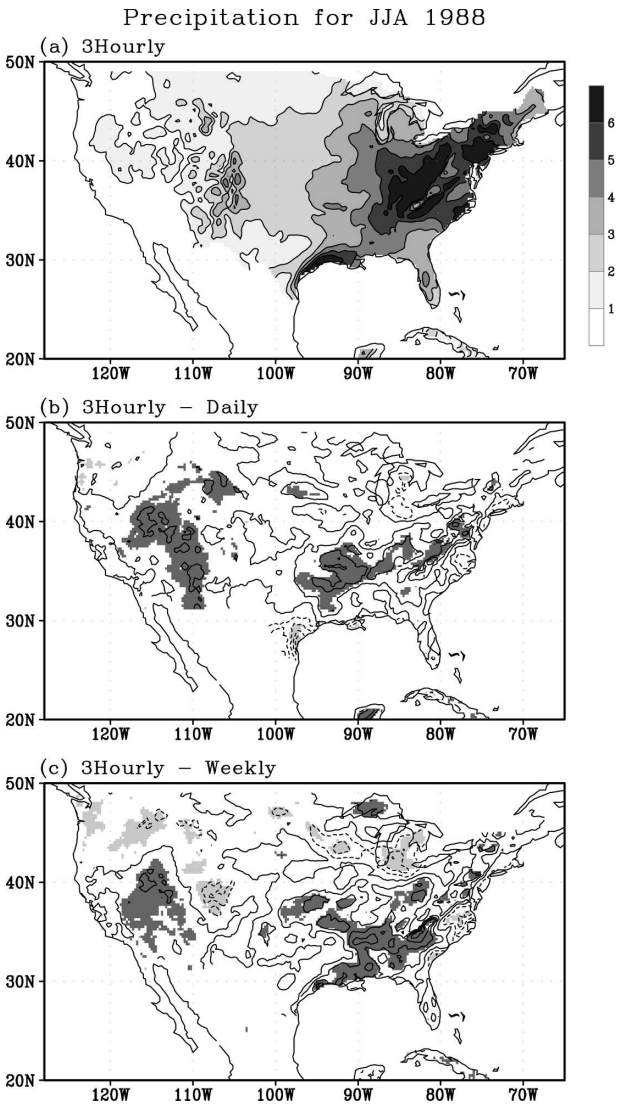

FIG. 6. (a) Pattern of Eta ensemble-mean precipitation (mm day^{-1}) simulated in experiments 3H for JJA 1988. (b) Difference in precipitation between experiments 3H and experiments D. (c) Difference in precipitation between experiments 3H and experiments W. In (b) and (c), significant values of 90% and higher confidence level of t test (with a decorrelation time scale of 3 days) are shaded and dashed contours are for negative values. Dark (light) shading is for significant positive (negative) values. (Contour intervals: 0.5.)

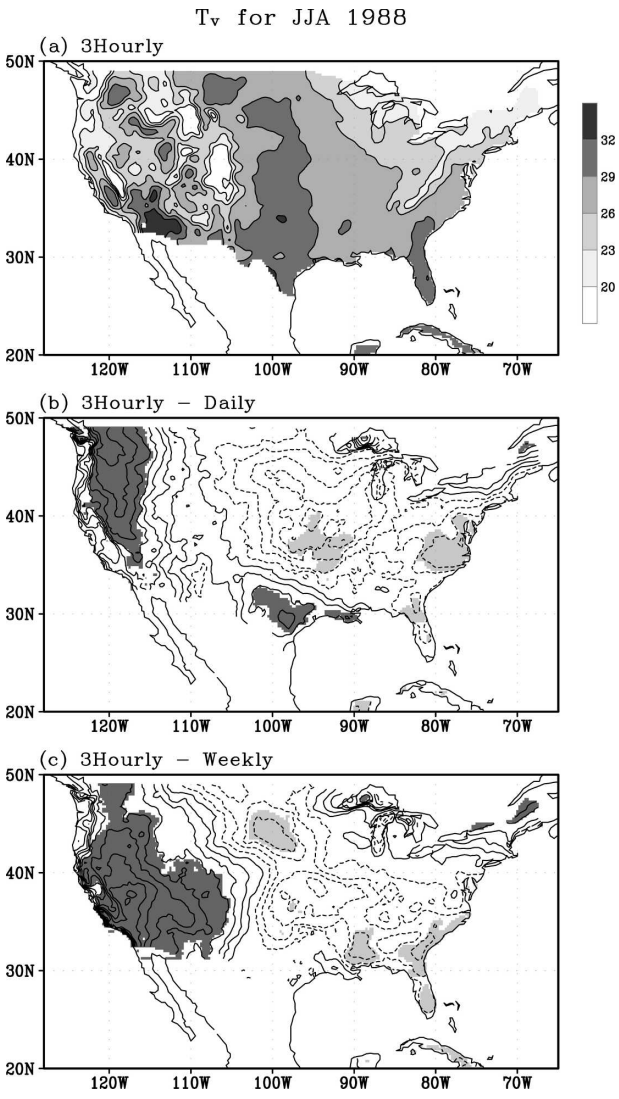

FIG. 7. (a) Pattern of Eta ensemble-mean 2-m virtual temperature (°C) simulated in experiments 3H for JJA 1988. (b) Difference in temperature between experiments 3H and experiments D. (c) Difference in temperature between experiments 3H and experiments W. In (b) and (c), significant values of 90% and higher confidence level of t test (with a decorrelation time scale of 3 days) are shaded and dashed contours are for negative values. (Contour intervals: 0.1.)

Figure 11 shows the seasonally averaged daily variances of precipitation and temperature and their changes with soil moisture forcing in various experiments for 1993. Compared to 1988, the daily precipitation variability is mostly smaller in 1993 except in the Pacific Northwest and the northern Midwest. However, besides the West Coast (including Nevada and Arizona), northern Midwest, and the Great Lakes, the patterns of temperature variance are similar between the two years. As in 1988, the high-frequency variability of soil moisture causes similar changes in mean precipitation and precipitation variance for 1993. Associated with the high-frequency variability of soil moisture, precipitation variance decreases in most of the Midwest, Southeast, and Ohio Valley (Figs. 11b,c) where the mean precipitation decreases (Figs. 9b,c). Again, as in 1988, there is no apparent relationship between mean temperature and temperature variance for 1993.

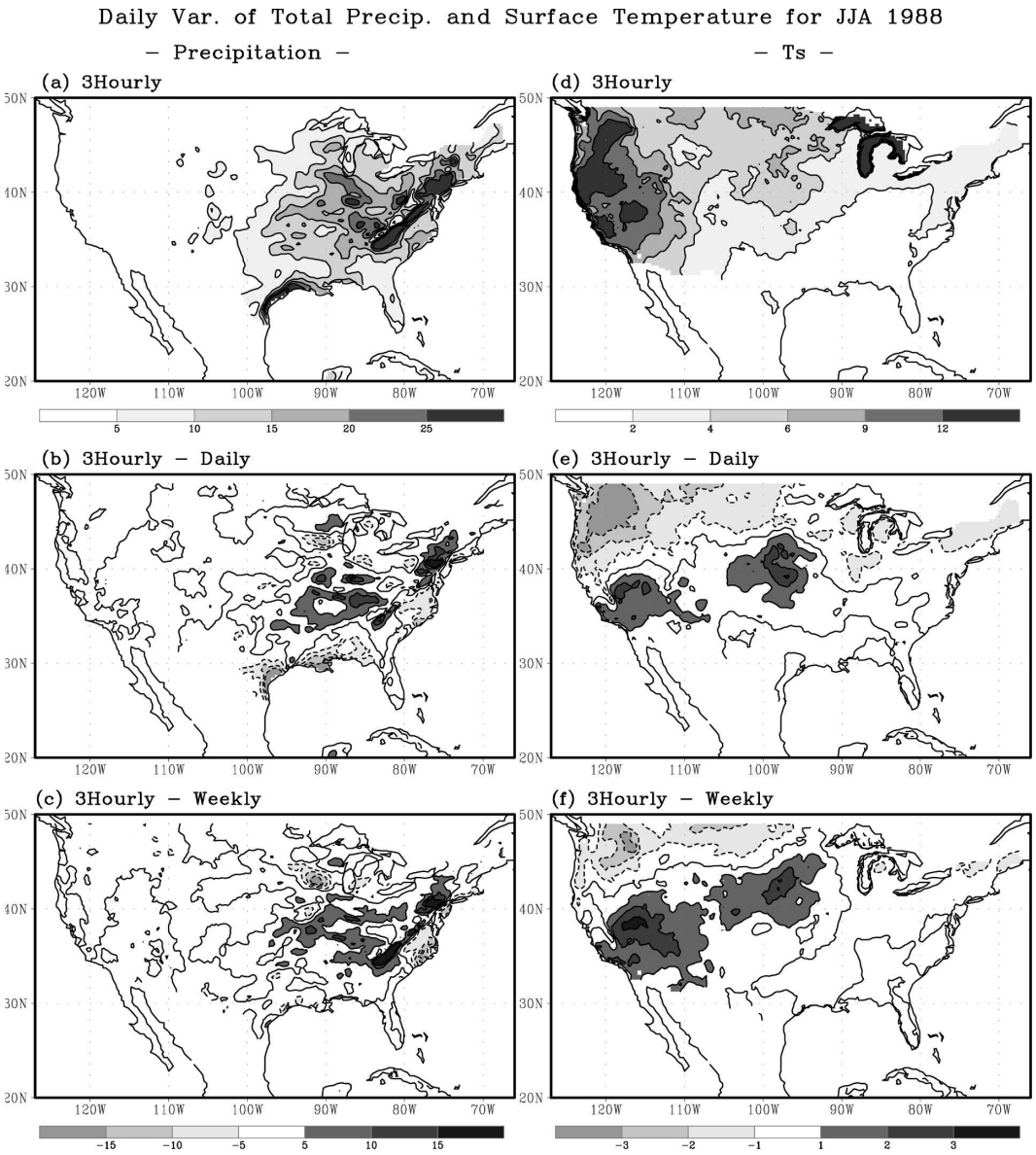

FIG. 8. (a) The daily variance of precipitation, in $(\text{mm day}^{-1})^2$, computed as the fluctuations from the seasonal means for JJA 1998. (b) Difference in precipitation variance between experiments 3H and experiments D. (c) Difference in precipitation variance between experiments 3H and experiments W. (d)–(f) Same as in (a)–(c), but for temperature variance in $(°C)^2$. In (b), (c), (e), and (f), zero contours are drawn and dashed contours are for negative values.

c. *Changes in evaporation and atmospheric circulation*

Here, we further analyze the patterns of evaporation and atmospheric circulation to understand the local and remote influences of the high-frequency variability of soil moisture.

1) YEAR OF 1988

Figure 12 shows the patterns of surface evaporation in experiments 3H and their differences in 3H-D and in 3H-W for JJA 1988. In experiments 3H (Fig. 12a), large evaporation appears in the eastern portion of the country, especially the Midwest, while small evaporation occurs in the southwestern and northern-central United States. The most striking feature of Fig. 12 is the increase in evaporation in experiments D and W in the central-eastern portion of the country (Figs. 12b,c). That is, the high-frequency variability of soil moisture increases the regional evaporation in 1988. There exist similar patterns of changes in evaporation, precipita-

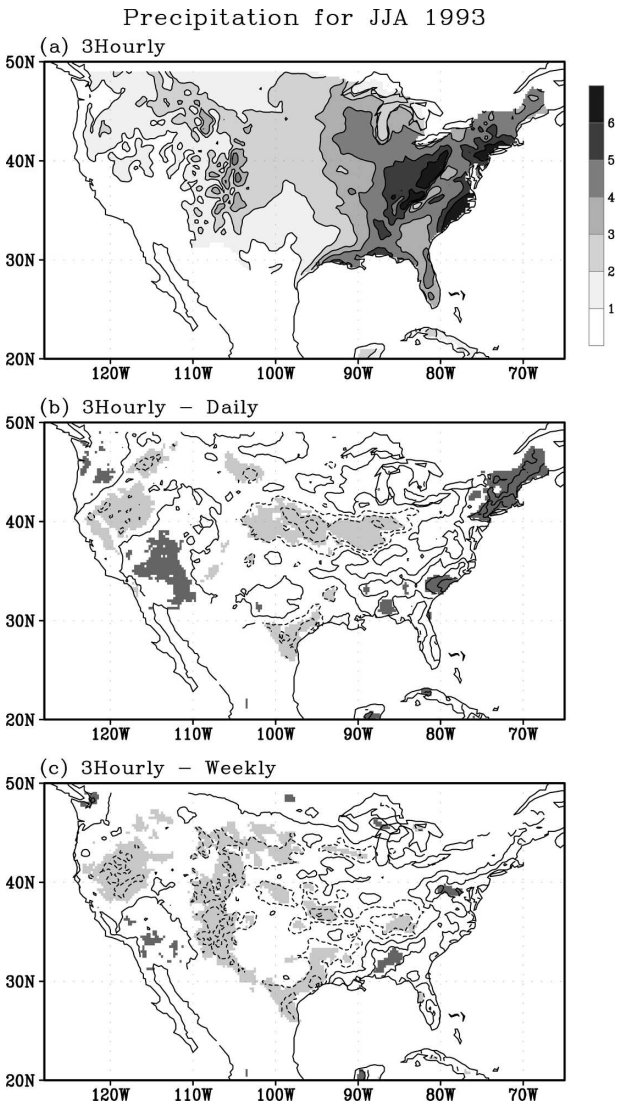

FIG. 9. Same as in Fig. 6, but for 1993.

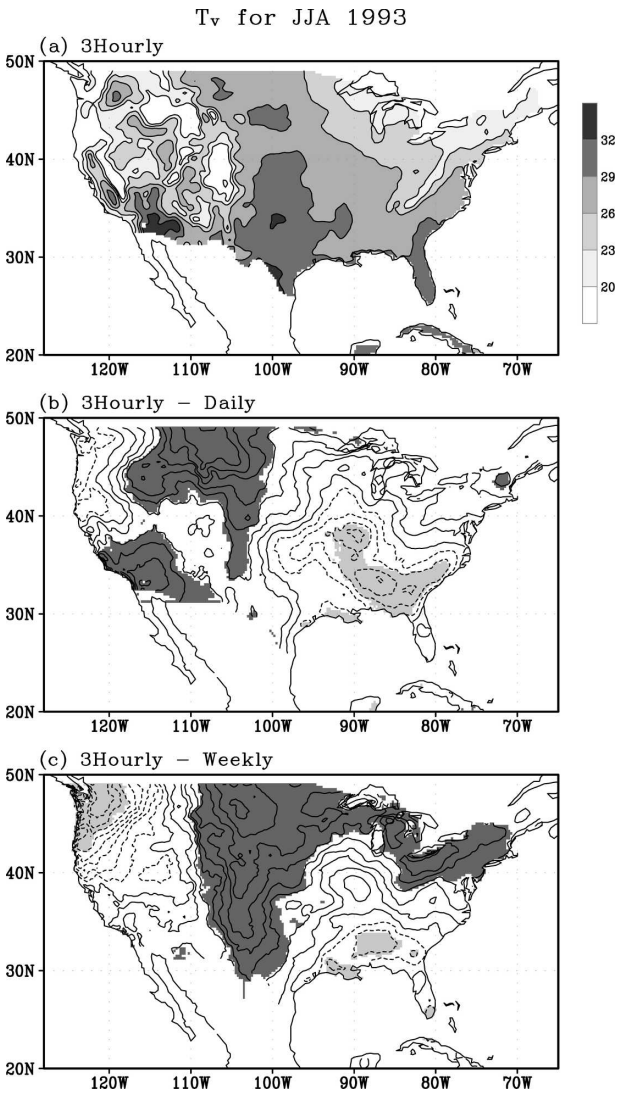

FIG. 10. Same as in Fig. 7, but for 1993.

tion, and temperature (see Figs. 12b,c; 6b,c; and 7b,c). These patterns show that enhancement (reduction) in evaporation is associated with increases (decreases) in precipitation and decreases (increases) in temperature for a large part of the country.

Since the local effect associated with evaporation feedback only explains about 10% of the changes in precipitation (cf. Figs. 6 and 12), we further examine the features of atmospheric circulation that are associated with the high-frequency variability of soil moisture. It can be seen from Fig. 13a, which shows the pattern of 850-mb winds of JJA 1988 in experiments 3H, that the Bermuda high controls the central and eastern portion of United States. It transports water vapor to the country mainly from the Gulf of Mexico and the Caribbean Sea. This major water vapor supply and its importance for the U.S. warm-season precipitation have been discussed in detail by Higgins et al. (1997) and Schubert et al. (1998), among many others. Water vapor is also transported, but relatively weakly, through the Southwest associated with the Northwesterly flow over the eastern Pacific.

Figures 13b and 13c reveal an important feature: The high-frequency variability of soil moisture increases water vapor transport from the western Atlantic Ocean and the Caribbean Sea to the central-eastern United States. This increase in water vapor transport is caused by the changes in the southerly flow west of the Bermuda high. Indeed, in both experiments D and W, especially in D, southerly wind weakens over the central-southern United States and the western Gulf of Mexico, and southerly–southeasterly flow strengthens

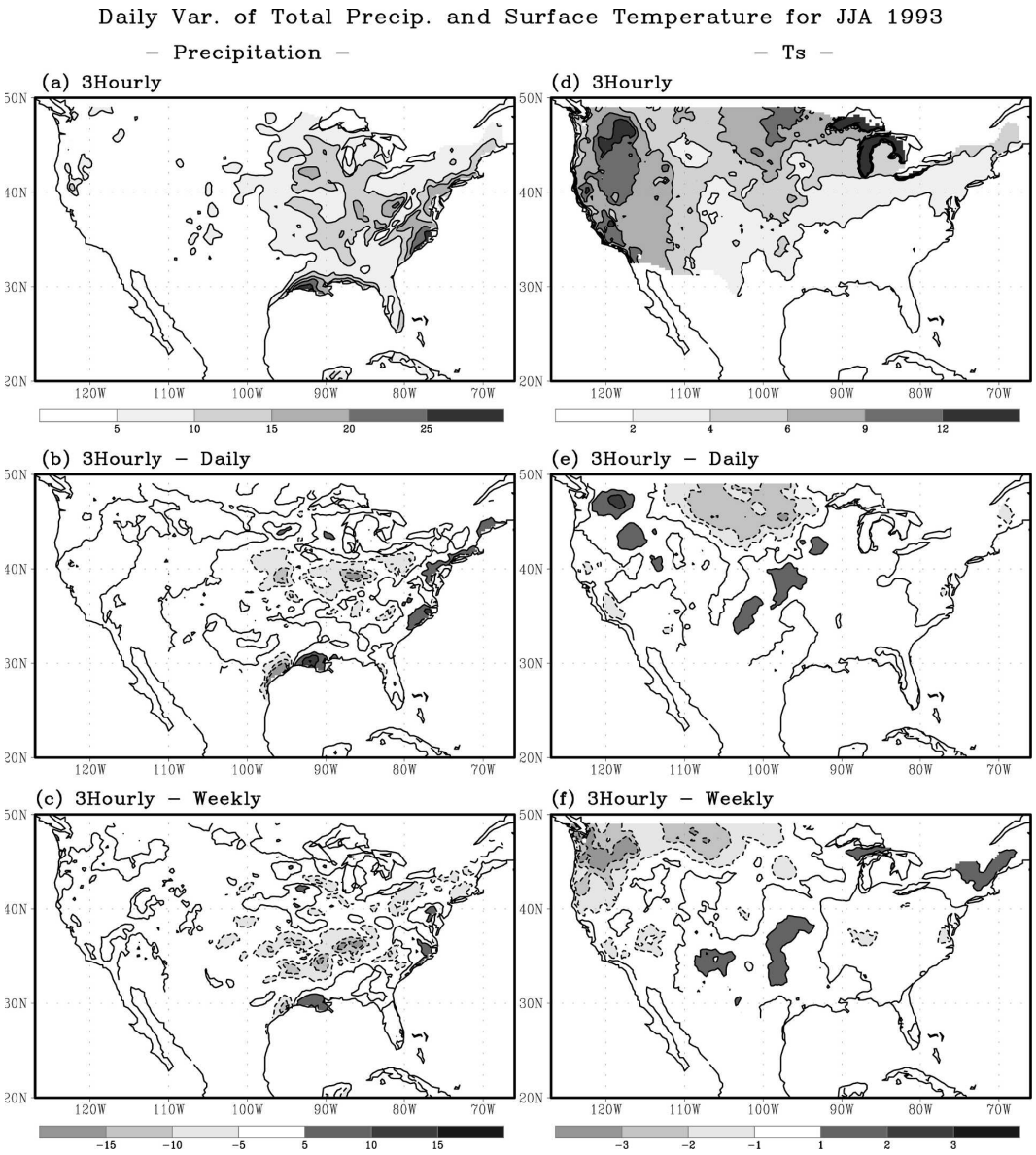

FIG. 11. Same as in Fig. 8, but for 1993.

to their east. An anomalous cyclonic pattern forms over the central United States (especially in Fig. 13b). Over the region of 30°–43°N and 75°–100°W, the inward low-level water vapor flux along 30°N and 75°W clearly outnumbers the outward flux along 43°N and 100°W, as shown in 3H-D. This convergence of the enhancing water vapor supply over the central-eastern United States largely accounts for the increase in precipitation shown in Figs. 6b,c.

2) YEAR OF 1993

Figure 14 shows the patterns of difference in evaporation between experiments 3H and D, and between 3H and W, for JJA 1993. Comparison of this figure with Figs. 9 and 10 indicates that wherever evaporation increases (decreases), precipitation generally increases (decreases) and temperature generally decreases (increases), with exceptions in the East Coast and especially in the Southeast for temperature. However, as in 1988, this local effect can only explain a small portion of changes in precipitation (e.g., cf. Figs. 9b and 12b).

The changes in atmospheric circulation patterns (Fig. 15) are also consistent with those in precipitation and temperature (Figs. 9 and 10) for 1993. Figure 15 indicates that the high-frequency variability of soil moisture causes divergence of water vapor over the central

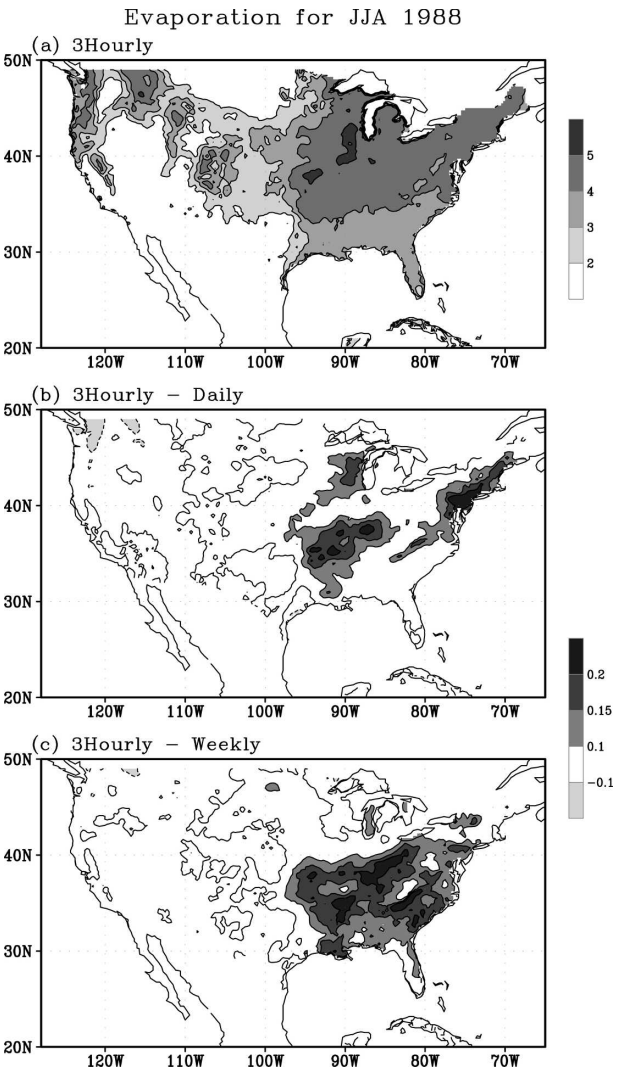

FIG. 12. (a) Pattern of Eta ensemble-mean surface evaporation (mm day^{-1}) simulated in experiments 3H for JJA 1988. (b) Difference in evaporation between experiments 3H and experiments D. (c) Difference in evaporation between experiments 3H and experiments W. In (b) and (c), zero contours are drawn and dashed contours are for negative values.

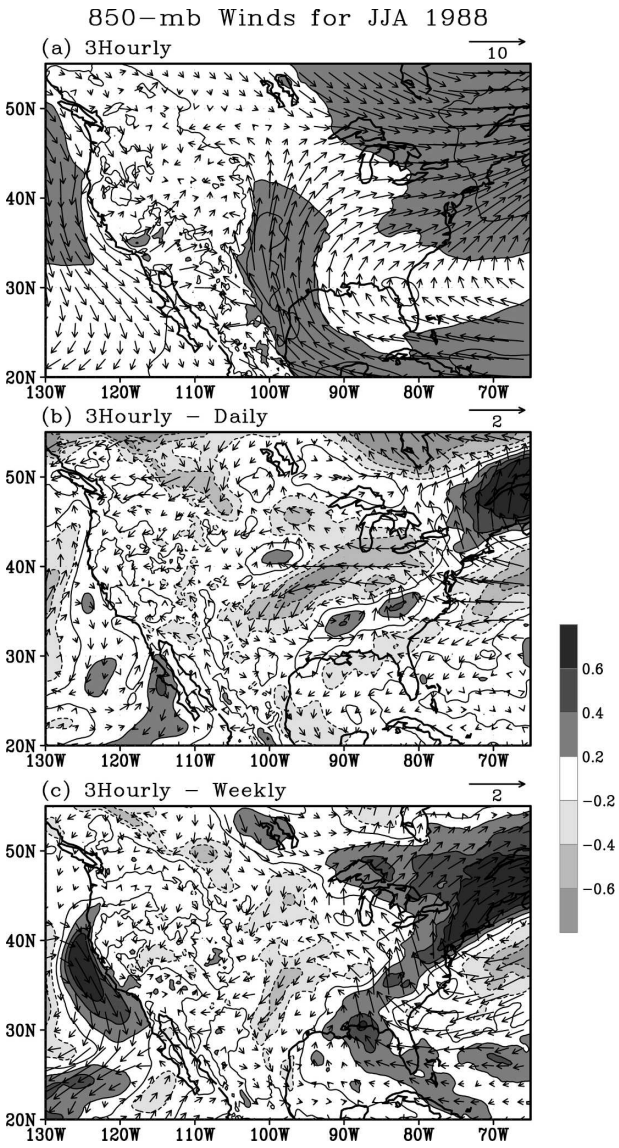

FIG. 13. (a) Pattern of Eta ensemble-mean 850-mb winds (m s^{-1}) simulated in experiments 3H for JJA 1988. (b) Difference in winds between experiments 3H and experiments D. (c) Difference in winds between experiments 3H and experiments W. The shading measures the magnitude of the winds. In (a), contour levels are 3, 5, and 7 and values larger than 5 m s^{-1} are shaded. In (b) and (c), zero contours are drawn and dashed contours are for negative values.

United States. Note the anomalous anticyclonic pattern centered about 40°N and the weakened southerly flow from the entire Gulf of Mexico, both of which decrease the precipitation over the central United States. The weakening in the southerly flow from the Gulf of Mexico also decreases the temperature over the Southeast shown in Fig. 10. Compared 3H to D, over the region of 33°–43°N and 85°–100°W, the maximum water vapor flux is the outward flux along 33°N. In addition, the diurnal and synoptic variability of soil moisture leads to anomalous southerly flow blowing from the western Atlantic Ocean to the northeastern United States, which increases the local precipitation and temperature.

4. Further discussions

It has been clearly demonstrated in the previous section that, in the Eta Model, the atmosphere responds strongly to the high-frequency variability of soil mois-

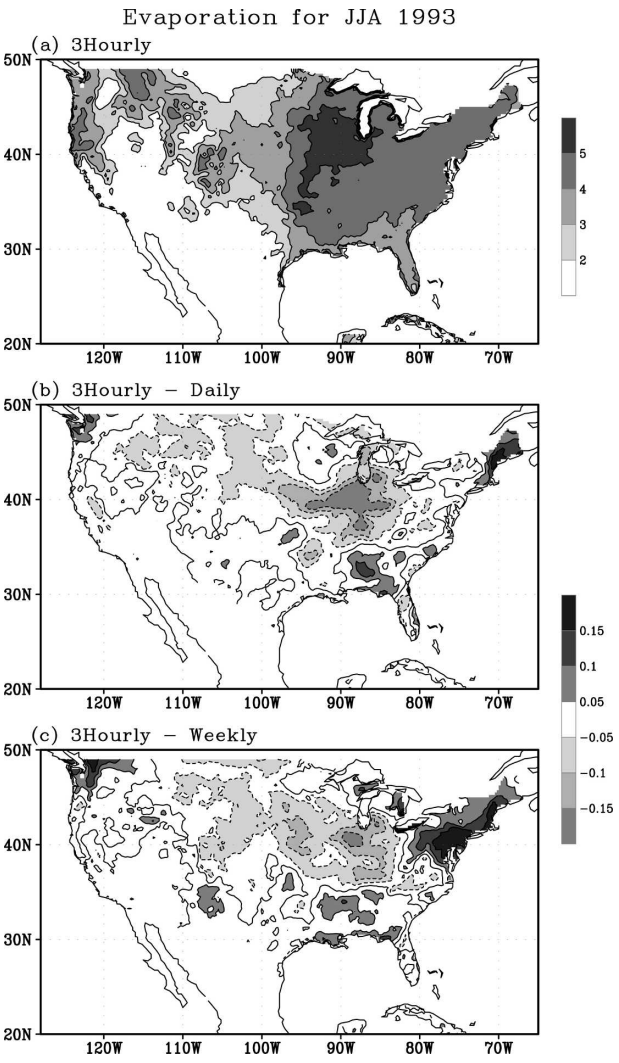

FIG. 14. Same as in Fig. 12, but for 1993.

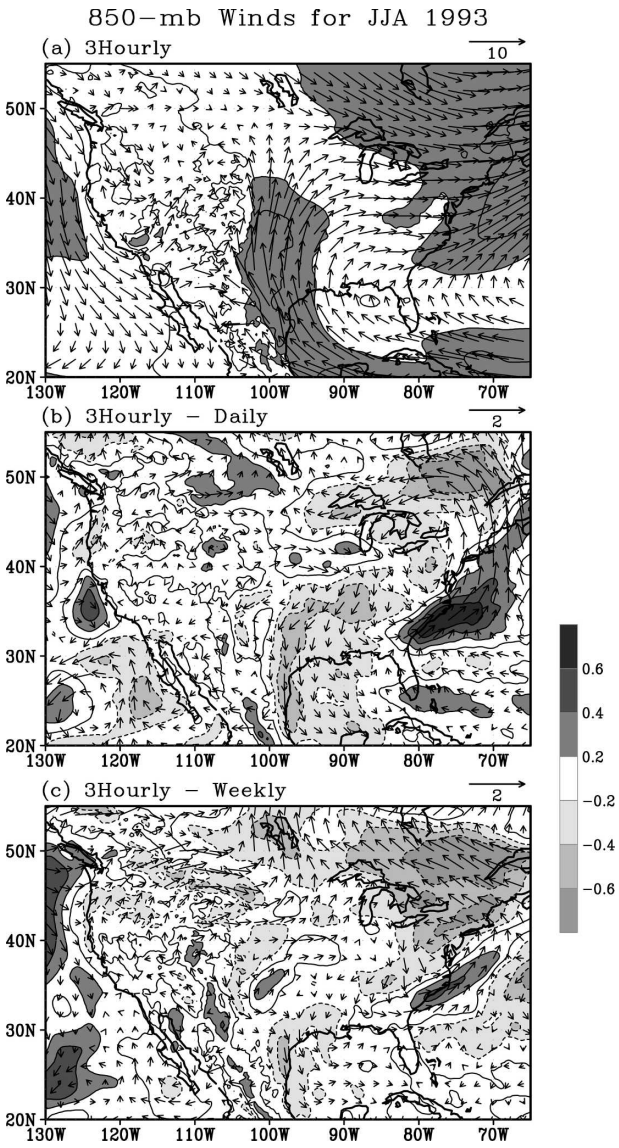

FIG. 15. Same as in Fig. 13, but for 1993.

ture. Large signals appear in the fields of precipitation, temperature, evaporation, and atmospheric circulation. Here, we further discuss the main features of the atmospheric response, the implication of the results for climate modeling, and the strengths and weaknesses of this study.

a. Importance of the diurnal cycle

This study has shown similar responses of the atmosphere to the diurnal variability and synoptic (including diurnal) variability of soil moisture, demonstrating the importance of the diurnal cycle of soil moisture. Among other commonly analyzed fields, temperature has strong diurnal cycles and it should be examined because of its close relationship with soil moisture. Figure 16 shows the patterns of differences in temperature, evaporation, and precipitation between the daytime (0300, 0600, 0900, and 1200 UTC) and nighttime (1500, 1800, 2100, and 0000 UTC) values for JJA 1988. In most of the United States, especially the eastern and central portion, the daytime temperature is significantly higher (Fig. 16a). When the temperature reaches its maximum in early afternoon, evaporation increases strongly (Fig. 16b) at the expense of soil moisture and thus precipitation increases (Fig. 16c). Here, we emphasize the importance of the rapid midday increase of surface temperature, which usually dominates over the changes in summertime temperature on the synoptic time scale.

However, the local effect described above associated with diurnal cycles should be complex and depend on

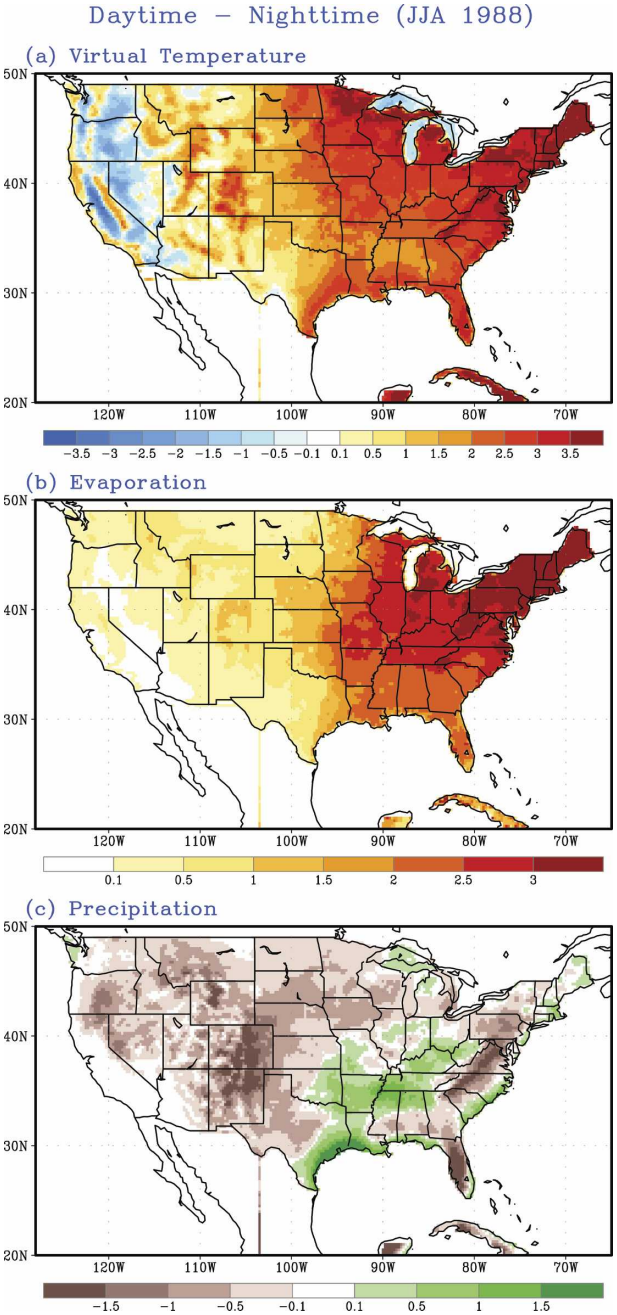

FIG. 16. Differences in (a) 2-m virtual temperature (°C), (b) evaporation (mm day^{-1}), and (c) precipitation (mm day^{-1}) between daytime and nighttime for JJA 1998. The values are from the ensemble means of experiments 3H. The daytime includes 0300, 0600, 0900, and 1200 UTC, and the nighttime includes 1500, 1800, 2100, and 0000 UTC.

many factors, such as the type of the soil and the amplitude of the diurnal cycles. As seen previously, it also competes with the remote influence of atmospheric circulation, which may be more vital for the issue addressed. We have also examined the daytime and nighttime patterns of temperature, evaporation, and precipitation for 1993 (figures not shown). However, we only obtain patterns largely similar to those shown in Fig. 16 and they are insufficient to explain the difference between the two years. This may partially be because the time interval of three hours applied in this study is not temporally fine enough to distinguish the differences in diurnal variability between the two years. Nevertheless, the feature echoes the lack of relationship between the mean temperature and temperature variance shown in Figs. 8 and 11.

b. *Spatial features*

As shown previously, apparent and consistent relationships between soil moisture, precipitation, and temperature occur mainly in the central and eastern portion of the United States. Over the western mountainous regions, the relationships between these fields become less apparent and even different from the relationships in the central-eastern country (see Figs. 6–11, 14, and 16). Topography and the type of land surface are among the many factors of these differences. In addition, in the coastal regions, the remote effect of atmospheric water transport is more influential than the local effect of evaporation feedback on the relationships between soil moisture, precipitation, and temperature. Also because of this remote effect, which is associated with the influence of SST, the changes in precipitation are more significant in the southern-tier states than in the northern-tier states of the United States (see Figs. 6 and 9).

c. *Implication of including high-frequency variability of soil moisture in models*

For all sensitivity experiments, we apply the soil moisture from the control simulations as surface boundary forcing, because experiments using observed or analyzed soil moisture such as that in NLDAS may not satisfy the requirement for water balance in the model. Because of the design of model experiments in this study, we assess the climate impact of high-frequency variability of soil moisture by comparing the results between the different experiments, instead of comparing the various model outputs with observations.

The large differences between the precipitation of control simulations and the precipitation of experiments D and W (compared to experiments 3H) indicate the need to include the diurnal variability of soil moisture in precipitation simulations. However, the response of precipitation to the diurnal cycle of soil moisture improves model performance only in some places,

while it fails to do so in others. Also, despite the fact that the Eta Model is one of the state-of-the-art regional climate models, there are substantial discrepancies between model outputs and observations (see section 3a) and these discrepancies hamper a clear understanding of the relationship between the diurnal cycle of soil moisture and improvement in climate modeling. Here, we conduct a further analysis of the performance of the model in simulating the diurnal cycle of soil moisture, the main forcing anomaly in our experiments, and its implication for modeling seasonal precipitation.

We apply the method used in Lee et al. (2007, see their appendix) to depict the amplitude and phase of the diurnal cycle of top-layer soil moisture in the Eta Model and NLDAS and estimate the statistical significance of the amplitude and phase of the diurnal cycle. (For the Eta Model, we first interpolate the 3-hourly model output into hourly values.) In this method, the amplitude and phase of the diurnal cycle of the observed and simulated soil moisture are defined by constructing a mean 24-h diurnal time series by averaging the soil moisture hour by hour over the entire period. This mean diurnal cycle is then decomposed using Fourier harmonic analysis to determine the amplitude and phase of the wavenumber-1 (24-h cycle) component. The significance of the estimated amplitude and phase is tested by describing the diurnal cycle in terms of Fourier components and examining their variance [see Lee et al. (2007) for details]. Figure 17 shows the local solar time that the maximum of the diurnal cycle of soil moisture appears for 1988. (Observed hourly soil moisture data for 1993 are not available at the time of this analysis.) It can be seen from Fig. 17a that the maximum of the 24-h cycle of soil moisture appears near midnight (local time) in the Southeast and a large area in the west. In most of the central and northeastern states, the maximum appears at 5–6 A.M. The Eta Model (Fig. 17b) captures the features of the phase of soil moisture diurnal cycle very well for many states but unrealistically for the Southeast and Northeast. Specifically, the maximum of the diurnal cycle of model soil moisture unrealistically occurs at 5–7 A.M. in the Southeast and around midnight in the Northeast. Thus, in places where the model captures the phase of the diurnal cycle of soil moisture correctly, it simulates the mean precipitation pretty well as for the northern Midwest (see Fig. 1). However, poor simulation of the phase of diurnal cycle appears in places where the model does not simulate the mean precipitation reasonably as seen in Fig. 1 for the Southeast.

Figure 18 shows the amplitude of the diurnal cycle of soil moisture in NLDAS and Eta. In the central and eastern United States (areas of interest of this study)

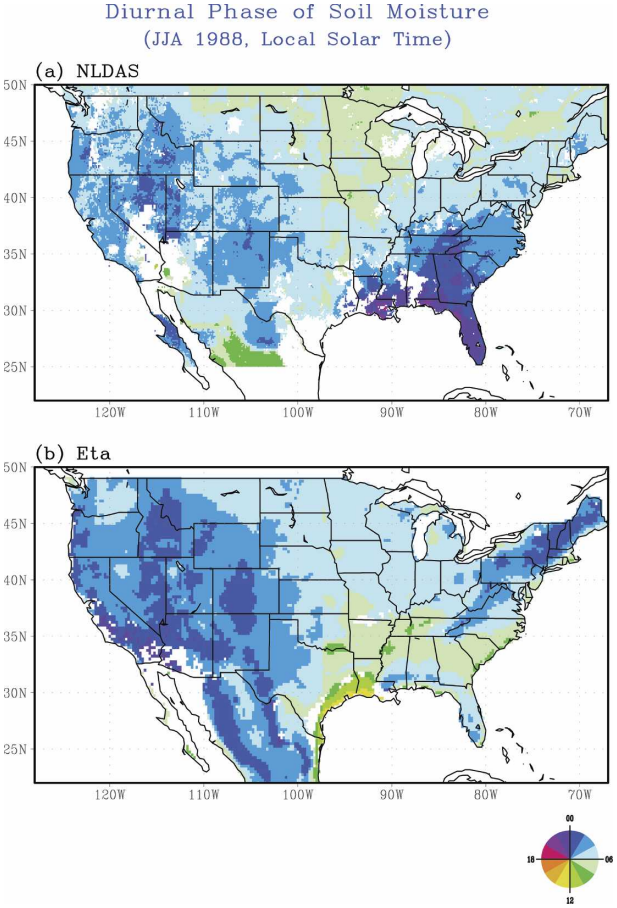

FIG. 17. Local solar time (h) of the maximum of the diurnal cycle of soil moisture in (a) NLDAS and (b) Eta as measured by hour indicated by the scale shown in the bottom right of the figure. Significant values exceeding the 95% confidence levels are shaded.

the model simulates the amplitude of the soil moisture diurnal cycle pretty well, especially in the Midwest. However, in the Southeast, especially the regions from Arkansas northeastward through Tennessee and Kentucky to West Virginia, the model clearly underestimates the amplitude of the diurnal cycle of soil moisture. Again, these regions are characterized by major differences in precipitation between the model and observations.

d. Strengths and weaknesses of the study

This study conducts innovative numerical experiments to investigate how the atmosphere responds to the high-frequency variability of soil moisture and focuses on the selective responses of the central-eastern U.S. hydroclimate to the diurnal and synoptic variability of soil moisture. Model integrations are extended to several months from previous studies using the Eta

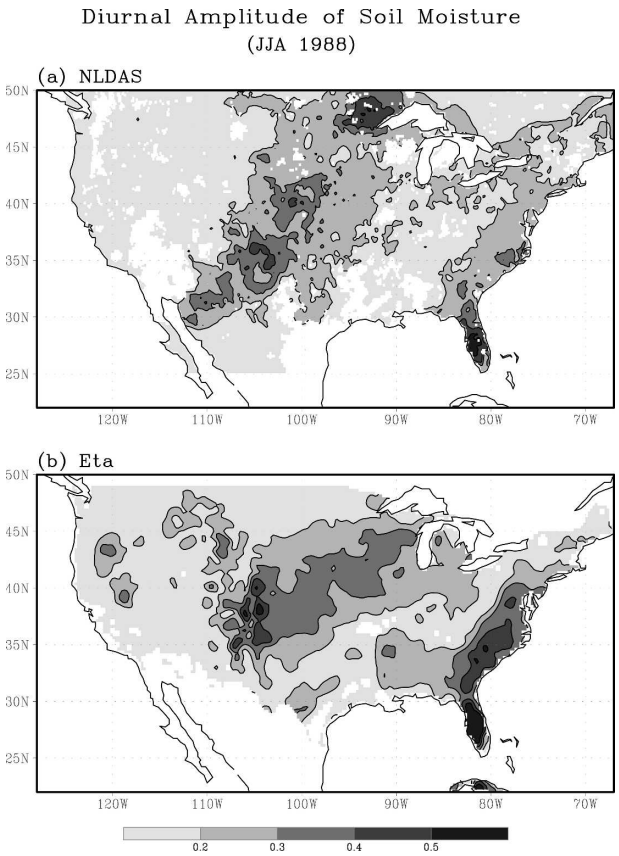

FIG. 18. Amplitude (mm day^{-1}) of the diurnal cycle of soil moisture in (a) NLDAS and (b) Eta computed from a harmonic analysis to the seasonal-mean diurnal time series. Significant values exceeding the 95% confidence levels are shaded.

Model, and all soil moisture forcings on different time scales are from the same data source. Thus, this work differs from previous studies (e.g., Betts et al. 1996; Fennessy and Shukla 1999; Pal and Eltahir 2001; Koster et al. 2004) that assess the importance of initial land state for precipitation and temperature simulation and prediction. In a sense, the current study provides a complementary analysis to those previous studies.

This study has revealed one particularly important feature: The diurnal cycle of soil moisture does matter in climate modeling, given the strong response in the fields of precipitation, temperature, and atmospheric circulation. However, the physical mechanisms for the atmospheric response to the diurnal cycle of soil moisture have not been fully explained, although we have analyzed the 3-hourly fields of temperature, evaporation, and precipitation and emphasized the importance of midday change in temperature for the changes in evaporation and soil moisture.

As demonstrated by the Global Land–Atmosphere Coupling Experiment (e.g., Dirmeyer et al. 2006; Guo et al. 2006; Koster et al. 2006), the current weather and climate models face tremendous difficulties in simulating the coupling between the land and the atmosphere. As put forward by Dirmeyer et al. (2006), most of the dozen participating models "do not encompass well the observed relationships between surface and atmospheric state variables and fluxes, suggesting that these models do not represent land-atmosphere coupling correctly." The strength of land–atmosphere coupling varies substantially from one model to another and exhibits large geographical variations within a given model.

The Eta Model is no different from the other models and its skill in climate simulation is at most marginal (e.g., Fennessy and Shukla 2000). As shown in section 3a, discrepancies between the model control simulations and observations are apparent in the current study, and we consider the long model integrations to be one of the factors causing these discrepancies, in addition to model inability itself. With regard to this model deficiency, two extreme points of view can be considered. The first is that hydrologically noteworthy years such as 1988 and 1993 are ultimately caused by the conditions of the oceans (positive feedback over land notwithstanding), so a respectable atmospheric model provided with correct SSTs should reproduce largely what happened in the real atmosphere. The other extreme view is that 1988 and 1993 are just single realizations of nature, and it is impossible to know to what extent the observed anomalies in specific years are boundary forced or mainly natural variability. Under this view, the Eta Model has succeeded in depicting the impact of soil moisture as long as we can find a model realization that matches reality approximately.

Figure 19 shows the difference patterns of JJA H500 between 1993 and 1988 for ensemble members using the initial conditions (ICs) of 27 April 1993 and 26 April 1988. Compared to the ensemble mean shown in Fig. 2, these specific realizations produce more realistic features. Accordingly, the precipitation and temperature fields (not shown) in these ensemble members are also better than those in the ensemble mean, indicating a dynamical consistency among different variables. However, the sensitivity of the atmosphere to the high-frequency variability of soil moisture (experiments 3H, W, and D) in these specific members is similar to that shown in Figs. 6 and 9 (for precipitation) and in Figs. 7 and 10 (for temperature). That is, the imperfection of the model control simulations does not significantly affect the major conclusions drawn by this study.

Nevertheless, the results obtained in this study need to be confirmed by future studies. Similar numerical experiments using different climate models and appli-

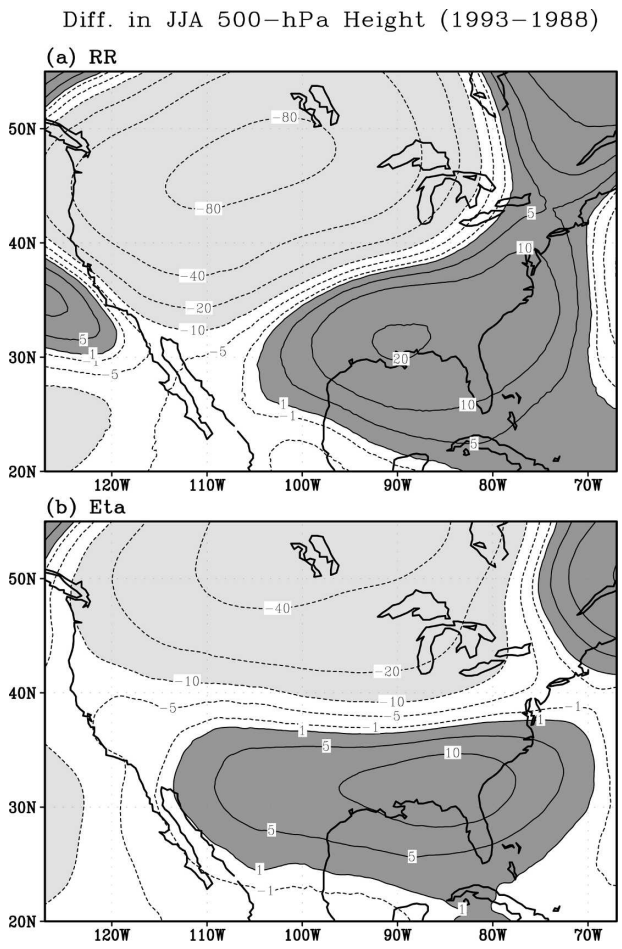

FIG. 19. Differences in JJA 500-mb geopotential height (m) between 1993 and 1988 in (a) the NCEP Regional Reanalysis and (b) a particular ensemble member of Eta control simulations.

cations of different microphysical schemes using the same model may provide useful information for improving our understanding of the impact of high-frequency variability of soil moisture on climate modeling. We have focused on the very different hydroclimate conditions and land surface processes in the summers of 1988 and 1993 when the large-scale SST forcing is also different (Niño-3.4 SST anomaly: −1.2 for 1988 and 0.5 for 1993). Although the degree of impact of moderate SST forcing on warm-season U.S. precipitation is still uncertain (e.g., Namias 1991; Trenberth and Guillemot 1996), it may be useful to conduct a similar study for neutral SST-forcing years. A fundamental problem for this and other studies has to do with prescribing soil moisture. In nature, soil moisture evolves interacting with the atmosphere and there is no guarantee that the prescribed soil moisture in models will necessarily yield correct atmospheric response.

5. Summary

In this study, we have applied a modified version of the NCEP Environmental Modeling Center Eta Model to investigate the response of the atmosphere to the high-frequency variability of soil moisture. We have focused on the influences of the diurnal and synoptic variability of soil moisture on the precipitation and temperature over the central-eastern United States in the summers of 1988 and 1993, and emphasized the importance of long-period integration of the model with a combination of the Betts–Miller convection scheme and the Noah land model, which thus far has mainly been applied for the purpose of operational weather forecasting.

High-frequency variability of soil moisture increases the precipitation in 1988 but decreases the precipitation in 1993, with major signals in the southern Midwest and the Southeast. Diurnal variability and synoptic variability of soil moisture cause similar changes in precipitation, indicating the importance of the diurnal cycle of land surface process. The increase (decrease) in precipitation is accompanied by a decrease (increase) in temperatures at the surface and the lower troposphere. The changes in precipitation and temperature are attributed to both local effect associated with evaporation feedback and remote influences associated with large-scale water vapor transport. The precipitation increase and temperature decrease in 1988 are accompanied by increase in evaporation and large-scale convergence of water vapor into the Midwest and Southeast. Consistent relationships are seen in 1993 when the high-frequency variability of soil moisture decreases evaporation and water vapor supply and thus reduces precipitation and increases temperature.

It is also found that, if the diurnal cycle of soil moisture is not included in the surface boundary forcing, the model precipitation differs apparently from that in the control simulations. In places of small difference between the simulated and observed precipitation, the model simulates the diurnal cycle of soil moisture reasonably well. However, the model fails to capture the diurnal cycle of soil moisture in regions where modeled precipitation is clearly different from the observed. These features demonstrate the importance of the diurnal cycle of soil moisture in climate modeling.

Acknowledgments. The authors thank Dr. Yun Fan for providing the NCEP Land Data Assimilation System soil moisture data, and Dr. Jongil Han for assistance in model experiments. Jon Gottschalck, Yun Fan, and three anonymous reviewers have provided helpful comments, which significantly improved the quality of

the manuscript. This study was supported by a NOAA/OGP GEWEX Americas Prediction Project.

REFERENCES

Baker, R. D., B. H. Lynn, A. Boone, W.-K. Tao, and J. Simpson, 2001: The influence of soil moisture, coastline curvature, and land-breeze circulations on sea-breeze-initiated precipitation. *J. Hydrometeor.,* **2,** 193–211.

Barnett, T. P., L. Dumenil, U. Schlese, E. Roecker, and M. Latif, 1989: The effect of Eurasian snow cover on regional and global climate variations. *J. Atmos. Sci.,* **46,** 661–685.

Beljaars, A. C. M., P. Viterbo, M. J. Miller, and A. K. Betts, 1996: The anomalies rainfall over the United States during July 1993: Sensitivity to land surface parameterization and soil moisture anomalies. *Mon. Wea. Rev.,* **124,** 362–383.

Betts, A. K., J. H. Ball, A. C. M. Beljaars, M. J. Miller, and P. A. Viterbo, 1996: The land surface–atmosphere interaction: A review based on observational and global modeling perspectives. *J. Geophys. Res.,* **101,** 7209–7225.

Chen, F., Z. I. Janjic, and K. E. Mitchell, 1997: Impact of atmospheric surface layer parameterization in the new land-surface scheme of the NCEP mesoscale Eta numerical model. *Bound.-Layer Meteor.,* **85,** 391–421.

Dirmeyer, P. A., A. J. Dolman, and N. Sato, 1999: The pilot phase of the global soil wetness project. *Bull. Amer. Meteor. Soc.,* **80,** 851–878.

——, F. J. Zeng, A. Ducharne, J. C. Morrill, and R. D. Koster, 2000: The sensitivity of surface fluxes to soil water content in three land surface schemes. *J. Hydrometeor.,* **1,** 121–134.

——, R. D. Koster, and Z. Guo, 2006: Do global models properly represent the feedback between land and atmosphere? *J. Hydrometeor.,* **7,** 1177–1198.

Ek, M. B., K. E. Mitchell, Y. Lin, E. Rogers, P. Grunmann, V. Koren, G. Gayno, and J. D. Tarpley, 2003: Implementation of the Noah land surface model advances in the National Centers for Environmental Prediction operational mesoscale Eta Model. *J. Geophys. Res.,* **108,** 8851, doi:10.1029/2002JD003296.

Eltahir, E. A. B., 1998: A soil moisture-rainfall feedback mechanism. I. Theory and observations. *Water Resour. Res.,* **34,** 765–776.

Fan, Y., H. M. Van den Dool, D. Lohmann, and K. Mitchell, 2006: 1948–98 U.S. hydrological reanalysis by the Noah Land Assimilation System. *J. Climate,* **19,** 1214–1237.

Fennessy, M. J., and J. Shukla, 1999: Impact of soil wetness on seasonal atmospheric prediction. *J. Climate,* **12,** 3167–3180.

——, and ——, 2000: Seasonal prediction over North America with a regional model nested in a global model. *J. Climate,* **13,** 2605–2627.

Guo, Z., and Coauthors, 2006: GLACE: The Global Land–Atmosphere Coupling Experiment. Part II: Analysis. *J. Hydrometeor.,* **7,** 611–625.

Gutowski, W. J., F. O. Otieno, R. W. Arritt, E. S. Takle, and Z. Pan, 2004: Diagnosis and attribution of a seasonal precipitation deficit in a U.S. regional climate simulation. *J. Hydrometeor.,* **5,** 230–242.

Gutzler, D. S., and J. W. Preston, 1997: Evidence for a relationship between spring snow cover in North America and summer precipitation in New Mexico. *Geophys. Res. Lett.,* **24,** 2207–2210.

Hahn, D. G., and J. Shukla, 1976: An apparent relationship between Eurasian snow cover and Indian monsoon rainfall. *J. Atmos. Sci.,* **33,** 2461–2462.

Higgins, R. W., Y. Yao, and X. L. Wang, 1997: Influence of the North American monsoon system on the U.S. summer precipitation regime. *J. Climate,* **10,** 2600–2622.

——, K. C. Mo, and Y. Yao, 1998: Interannual variability of the United States summer precipitation regime with emphasis on the Southwest Monsoon. *J. Climate,* **11,** 2582–2606.

——, W. Shi, and E. Yarosh, 2000: *Improved United States Precipitation Quality Control System and Analysis.* NCEP/Climate Prediction Center Atlas 7, 40 pp.

Hong, S.-Y., and E. Kalnay, 2000: Role of sea surface temperature and soil-moisture feedback in the 1998 Oklahoma–Texas drought. *Nature,* **408,** 842–844.

Hu, Q., and S. Feng, 2002: Interannual rainfall variations in the North American summer monsoon region: 1900–98. *J. Climate,* **15,** 1189–1202.

Huang, J., and H. M. Van den Dool, 1993: Monthly precipitation–temperature relations and temperature prediction over the United States. *J. Climate,* **6,** 1111–1132.

——, ——, and K. P. Georgakakos, 1996: Analysis of model-calculated soil moisture over the United States (1931–1993) and applications to long-range temperature forecasts. *J. Climate,* **9,** 1350–1362.

Janjić, Z. I., 1990: The step-mountain coordinate: Physical package. *Mon. Wea. Rev.,* **118,** 1429–1443.

——, 1994: The step-mountain Eta coordinate model: Further developments of convection, viscous sublayer, and turbulence closure schemes. *Mon. Wea. Rev.,* **122,** 927–945.

Kanamitsu, M., W. Ebisuzaki, J. Woollen, S.-K. Yang, J. J. Hnilo, M. Fiorino, and G. L. Potter, 2002: NCEP–DOE AMIP-II reanalysis (R-2). *Bull. Amer. Meteor. Soc.,* **83,** 1631–1643.

Koster, R. D., and M. J. Suarez, 1995: The relative contributions of land and ocean processes to precipitation variability. *J. Geophys. Res.,* **100,** 13 775–13 790.

——, ——, and M. Heiser, 2000: Variance and predictability of precipitation at seasonal-to-interannual timescales. *J. Hydrometeor.,* **1,** 26–46.

——, and Coauthors, 2004: Realistic initialization of land surface states: Impacts on subseasonal forecast skill. *J. Hydrometeor.,* **5,** 1049–1063.

——, and Coauthors, 2006: GLACE: The Global Land–Atmosphere Coupling Experiment. Part I: Overview. *J. Hydrometeor.,* **7,** 590–610.

Lau, K.-M., and W. R. Bua, 1998: Mechanisms of monsoon–Southern Oscillation coupling: Insights from GCM experiments. *Climate Dyn.,* **14,** 759–779.

Lee, M.-I., and Coauthors, 2007: Sensitivity of horizontal resolution in the AGCM simulations of warm season diurnal cycle of precipitation over the United States and northern Mexico. *J. Climate,* **20,** 1862–1881.

Mahanama, S. P. P., and R. D. Koster, 2005: AGCM biases in evaporation regimes: Impacts on soil moisture memory and land–atmosphere feedback. *J. Hydrometeor.,* **6,** 656–669.

Meehl, G. A., 1994: Influence of the land surface in the Asian summer monsoon: External conditions versus internal feedbacks. *J. Climate,* **7,** 1033–1049.

Mellor, G. L., and T. Yamada, 1982: Development of a turbulence closure model for geophysical fluid problems. *Rev. Geophys. Space Phys.,* **20,** 851–875.

Mesinger, F., and Coauthors, 2006: North American Regional Reanalysis. *Bull. Amer. Meteor. Soc.,* **87,** 343–360.

Namias, J., 1991: Spring and summer 1988 drought over the contiguous United States—Causes and prediction. *J. Climate,* **4,** 54–65.

Pal, J. S., and E. A. B. Eltahir, 2001: Pathways relating soil moisture conditions to future summer rainfall within a model of the land–atmosphere system. *J. Climate,* **14,** 1227–1242.

——, and ——, 2002: Teleconnections of soil moisture and rainfall during the 1993 midwest summer flood. *Geophys. Res. Lett.,* **29,** 1865, doi:10.1029/2002GL014815.

Palmer, T. N., and Coauthors, 2004: Development of a European multimodel ensemble system for seasonal-to-interannual prediction (DEMETER). *Bull. Amer. Meteor. Soc.,* **85,** 853–872.

Qu, W., and Coauthors, 1998: Sensitivity of latent heat flux from PILPS land-surface schemes to perturbations of surface air temperature. *J. Atmos. Sci.,* **55,** 1909–1927.

Saha, S., and Coauthors, 2006: The NCEP Climate Forecast System. *J. Climate,* **19,** 3483–3517.

Schubert, S. D., H. M. Helfand, C. Y. Wu, and W. Min, 1998: Subseasonal variations in warm-season moisture transport and precipitation over the central and eastern United States. *J. Climate,* **11,** 2530–2555.

Segal, M., R. W. Arritt, C. Clark, R. Rabin, and J. Brown, 1995: Scaling evaluation of the effect of surface characteristics of potential for deep convection over uniform terrain. *Mon. Wea. Rev.,* **123,** 383–400.

Smith, C. B., M. N. Lakhtakia, W. J. Capehart, and T. N. Carlson, 1994: Initialization of soil-water content in regional scale atmospheric prediction models. *Bull. Amer. Meteor. Soc.,* **75,** 585–593.

Stern, W., and K. Miyakoda, 1995: Feasibility of seasonal forecasts inferred from multiple GCM simulations. *J. Climate,* **8,** 1071–1085.

Takle, E. S., and Coauthors, 1999: Project to intercompare regional climate simulations (PIRCS): Description and initial results. *J. Geophys. Res.,* **104,** 19 443–19 461.

Timbal, B., S. Power, R. Colman, J. Viviand, and S. Lirola, 2002: Does soil moisture influence climate variability and predictability over Australia? *J. Climate,* **15,** 1230–1238.

Trenberth, K. E., and C. J. Guillemot, 1996: Physical processes involved in the 1988 drought and 1993 floods in North America. *J. Climate,* **9,** 1288–1298.

Viterbo, P., and A. K. Betts, 1999: Impact of the ECMWF reanalysis soil water on forecast of the July 1993 Mississippi flood. *J. Geophys. Res.,* **104,** 19 361–19 366.

Weaver, C. P., 2004: Coupling between large-scale atmospheric processes and mesoscale land-atmosphere interactions in the U.S. southern Great Plains during summer. Part II: Mean impacts of the mesoscale. *J. Hydrometeor.,* **5,** 1247–1258.

Xue, Y., F. J. Zeng, and C. A. Schlosser, 1996: SSiB and its sensitivity to soil properties—A case study using HAPEX-Mobilhy data. *Global Planet. Change,* **13,** 183–194.

——, ——, K. E. Mitchell, Z. Janjic, and E. Rogers, 2001: The impact of land surface processes on simulations of the U.S. hydrological cycle: A case study of 1993 flood using the SSiB Land Surface Model in the NCEP Eta Regional Model. *Mon. Wea. Rev.,* **129,** 2833–2860.

Yang, S., and K.-M. Lau, 1998: Influences of sea surface temperature and ground wetness on Asian summer monsoon. *J. Climate,* **11,** 3230–3246.

——, and ——, 2006: Interannual variability of the Asian monsoon. *The Asian Monsoon,* B. Wang, Ed., Praxis, 259–293.

——, ——, and M. Sankar-Rao, 1996: Precursory signals associated with the interannual variability of the Asian summer monsoon. *J. Climate,* **9,** 949–964.

Zhao, Q., and F. H. Carr, 1997: A prognostic cloud scheme for operational NWP models. *Mon. Wea. Rev.,* **125,** 1931–1953.

Zhu, J., and X.-Z. Liang, 2005: Regional climate model simulation of U.S. soil temperature and moisture during 1982–2002. *J. Geophys. Res.,* **110,** D24110, doi:10.1029/2005JD006472.